Penerbit Akademia Baru

CFD Letters

Journal homepage: www.akademiabaru.com/cfdl.html
ISSN: 2180-1363

Stagnation Point Flow of Hybrid Nanofluid over a Permeable Vertical Stretching/Shrinking Cylinder with Thermal Stratification Effect

Open Access

Najiyah Safwa Khashi'ie[1,2,*], Ezad Hafidz Hafidzuddin[3], Norihan Md Arifin[1,4], Nadihah Wahi[4]

[1] Institute for Mathematical Research, Universiti Putra Malaysia, 43400 UPM Serdang, Selangor, Malaysia
[2] Fakulti Teknologi Kejuruteraan Mekanikal dan Pembuatan, Universiti Teknikal Malaysia Melaka, Hang Tuah Jaya, 76100, Durian Tunggal, Melaka, Malaysia
[3] Centre of Foundation Studies for Agricultural Science, Universiti Putra Malaysia, 43400 UPM Serdang, Selangor, Malaysia
[4] Department of Mathematics, Faculty of Science, Universiti Putra Malaysia, 43400 UPM Serdang, Selangor, Malaysia

ARTICLE INFO

Article history:
Received 22 December 2019
Received in revised form 18 February 2020
Accepted 23 February 2020
Available online 29 February 2020

Keywords:
Hybrid nanofluid; stagnation point flow; stretching/shrinking cylinder; thermal stratification; dual solutions

ABSTRACT

Hybrid nanofluid is invented to improve the heat transfer performance of traditional working fluids (water, traditional nanofluid) in many engineering applications. The present study highlights the numerical solutions and stability analysis of stagnation point flow using hybrid nanofluid over a permeable stretching/shrinking cylinder. The combination of copper (Cu) and alumina (Al_2O_3) nanoparticles with water as the base fluid is analytically modeled using the single phase model and modified thermophysical properties. A set of transformation is adopted to reduce the complexity of the governing model and then, numerically computed using the bvp4c solver in Matlab software. Suction parameter is vital to generate dual similarity solutions in shrinking cylinder case while no solution is found if the surface is impermeable. Two solutions are possible for the assisting and opposing flow within a specific value of the buoyancy parameter. For the shrinking cylinder, Al_2O_3-water nanofluid has the lowest heat transfer rate than Cu-water and hybrid Cu-Al_2O_3/water nanofluids. A suitable combination of alumina and copper nanoparticles volumetric concentration in hybrid nanofluid can produce higher heat transfer rate than the Cu-water nanofluid. The execution of stability analysis reveals that the first solution is more realistic than second solution. However, the present results are only fixed to the combination of copper and alumina nanoparticles only and the other kind of hybrid nanofluid may have different outcomes.

1. Introduction

Hybrid nanofluid is a new procreation of heat transfer fluid which may provide better heat transfer performance as compared to the traditional cooling fluid (water, ethylene glycol) and nanofluid (single nanoparticle). There are many review papers which discussed the significance of hybrid nanofluids in industrial and technological sectors [1-8], the preparation and stability of the

* *Corresponding author.*
E-mail address: najiyah@utem.edu.my (Najiyah Safwa Khashi'ie)

hybrid nanoparticles. Among of the factors to create a stable hybrid nanofluid is by selecting a good combination of nanoparticles. The commonly used nanoparticles were categorized into these groups; metals (Cu, Ag), metal oxides (Al_2O_3, CuO, Fe_2O_3), carbon materials (graphite, MWCNTs, CNTs), metal carbide and metal nitride. Besides, the size, shape and solid volume fractions of the nanoparticles are also the important factors to optimize the thermal conductivity of the hybrid nanofluid. The mathematical models by Buongiorno [9] and Tiwari and Das [10] are frequently used in the formulation of boundary layer flow in nanofluid. Khashi'ie *et al.,* [11,12] used Buongiorno model to scrutinize the impact of double stratification on heat and mass transfer due to a permeable and deformable flat plate. Other recent investigations on stretching flow using Buongiorno model can be found in Rabbi *et al.,* [13,14], Rana *et al.,* [15] and Khan *et al.,* [16]. Devi and Devi [17] introduced the thermophysical properties to represent hybrid nanofluid, and then adopted them into the existing Tiwari and Das model. They also revealed that the heat transfer rate of Cu-Al_2O_3/water hybrid nanofluid was greater than Cu-water nanofluid under magnetic field environment and low suction strength $(0 \leq S \leq 1.5)$.

Stagnation point flow is generally referred to the flow which contact the solid surface and consequently, separate into two different regions. This kind of flow has extensively been applied in the industrial and technological sectors since it has optimum heat transfer, fluid pressure and mass deposition rate around the stagnation point region. Hiemenz [18] and Homann [19] were the earliest in the classical works of the stagnation point flow. The stagnation point flow due to a stretching flat plate was first considered by Chiam [20] while Wang [21] considered shrinking sheet and obtained two solutions. The duality of solutions identified by Wang [21] was validated by Awaludin *et al.,* [22], and they showed that the first solution was the real solution using the stability analysis. The studies on the stagnation point flow towards deformable flat plate were later conducted by Khashi'ie *et al.,* [23], Nasir *et al.,* [24-26] and Kamal *et al.,* [27,28] using viscous fluid and Khashi'ie *et al.,* [29,30] using traditional and hybrid nanofluids, respectively. Rostami *et al.,* [31] observed dual solutions for the stagnation point flow of silica-alumina/water hybrid nanofluid towards a vertical and static plate. However, due to the advancement in engineering and industrial sectors, fluid flow towards different surfaces such as disc, wedge and cylinder were further investigated. The analysis of hybrid nanofluid flow and heat transfer induced by stretching/shrinking disc and wedge were examined by Khashi'ie *et al.,* [32] and Waini *et al.,* [33], accordingly. The dual nature solutions were feasible when a suction parameter was imposed in both studies.

Early work on exterior fluid flow towards a stretching cylinder was conducted by Wang [34] while Ishak and Nazar [35] obtained a similarity solution for laminar boundary layer flow of a viscous fluid along a stretching cylinder. Poply *et al.,* [36] obtained dual solutions and conducted stability analysis for the MHD outer velocity flow of a viscous and incompressible fluid. Meanwhile, Vinita and Poply [37] analyzed the MHD slip flow with heat generation and outer velocity using Buongiorno's model of nanofluid. Mixed convective boundary layer flow with prescribed surface heat flux over a vertical cylinder was studied by Ishak [38] for impermeable cylinder and by Bachok and Ishak [39] for permeable cylinder. Ishak [38] found dual solutions for both buoyancy assisting and opposing flows and showed that the application of cylindrical surface could delay the boundary layer separation as compared to a flat sheet or plate. Arifuzzaman *et al.,* [40] analyzed the heat and mass transfer of natural convective flow in fourth-grade radiative fluid. Later, Khashi'ie *et al.,* [41] investigated the hybrid nanofluid flow past a permeable vertical cylinder with thermal stratification effect and attained two solutions. The stagnation point flow towards a stretching/shrinking cylinder was considered by Najib *et al.,* [42] for viscous fluid and Omar *et al.,* [43] for Cu-water nanofluid. Recently, Nadeem *et al.,* [44] studied three dimensional stagnation point flow over a static cylinder and dual

solutions were found. They also proved that the heat transfer rate of Cu-Al_2O_3/water hybrid nanofluid was greater as compared to the Cu-water nanofluid.

Inspired by all the previous literatures, the main idea of the present work is to numerically study the simultaneous effects of mixed convection and thermal stratification on the stagnation point flow of hybrid nanofluid towards a stretching/shrinking cylinder. The thermal stratification phenomenon is assumed with the usage of variable (non-constant) ambient temperature while the surface is permeable to enhance the flow due to the shrinking cylinder. In the study, the combination of copper (Cu) and alumina (Al_2O_3) is used. The governing model (partial differential equations) are converted into nonlinear ordinary differential equation using a set of similarity transformations and then, numerically computed using the boundary value problem solver (bvp4c) in Matlab software. Since all the previous literatures showed the existence of dual similarity solutions for the shrinking case, the present work also proposes the stability analysis to prove the physical (real) solution. All the authors are confident that there are no other literatures reported the present work.

2. Methodology

The present work deals with the stagnation point flow of a hybrid nanofluid towards a vertical permeable stretching/shrinking cylinder as portrayed in Figure 1. The cylinder with radius R is assumed to move with a linear velocity, $u_w(x) = \frac{ax}{L}$ while the free stream velocity is $u_e(x) = \frac{bx}{L}$ where L is the characteristic length of the cylinder and b is a positive constant. The permeable surface is important to maintain and enhance the flow due to shrinking cylinder. The fluid velocities are denoted by u and v which are measured in the $x-$ and $r-$ axes, respectively.

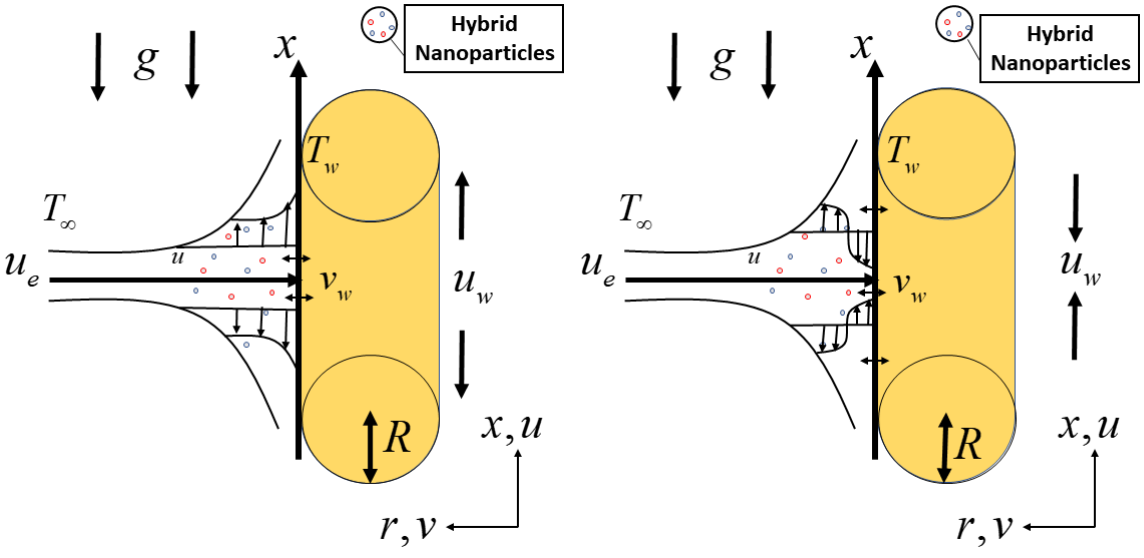

Fig. 1. The physical model with coordinate system for (a) stretching cylinder (b) shrinking cylinder

Since the mixed effects of convective flow and thermal stratification are incorporated in the study, the variable wall temperature, $T_w(x) = T_0 + \frac{Ax}{L}$ with linear stratified ambient temperature, $T_\infty(x) = T_0 + \frac{Bx}{L}$ are used where T_0 is the initial ambient temperature of the hybrid nanofluid, A is the characteristic temperature of the cylinder and $B > 0$.

Under all these assumptions, the mathematical model for the governing problem is (see Najib *et al.,* [42] and Omar *et al.,* [43])

$$\frac{\partial(ru)}{\partial x}+\frac{\partial(rv)}{\partial r}=0, \tag{1}$$

$$u\frac{\partial u}{\partial x}+v\frac{\partial u}{\partial r}=u_e\frac{du_e}{dx}+\frac{\mu_{hnf}}{\rho_{hnf}}\left(\frac{\partial^2 u}{\partial r^2}+\frac{1}{r}\frac{\partial u}{\partial r}\right)+\frac{(\rho\beta_T)_{hnf}g(T-T_\infty)}{\rho_{hnf}}, \tag{2}$$

$$u\frac{\partial T}{\partial x}+v\frac{\partial T}{\partial r}=\left(\frac{k}{\rho C_p}\right)_{hnf}\left(\frac{\partial^2 T}{\partial r^2}+\frac{1}{r}\frac{\partial T}{\partial r}\right), \tag{3}$$

along with the initial and boundary conditions

$$u(x,r)=u_w(x), v(x,r)=v_w, T(x,r)=T_w(x) \text{ when } r=R, \tag{4}$$

$$u(x,r)\to u_e(x), T(x,r)=T_\infty(x) \text{ when } r\to\infty. \tag{5}$$

T is the hybrid nanofluid temperature, g represents the gravitational acceleration while the dynamic viscosity, density, thermal expansion, thermal conductivity and specific heat of hybrid nanofluid are symbolized by $\mu_{hnf,}\ \rho_{hnf,}\ (\beta_T)_{hnf,}\ k_{hnf}$ and $(\rho C_p)_{hnf}$, respectively. For the numerical computation, $\rho_{hnf,}\ (\rho C_p)_{hnf}$, $\mu_{hnf,}\ k_{hnf}$ and $(\rho\beta_T)_{hnf}$ will be substituted with the expressions as presented in Table 1. Table 1 also specifies the comparison of the thermophysical properties between hybrid nanofluid and nanofluid (single nanoparticle). Further, the wall mass transfer equation for the permeable cylinder is $v_w=-\sqrt{\frac{bv_f}{L}}\left(\frac{R}{r}\right)S$ where wall mass suction for $v_w<0$ and injection for $v_w>0$.

A set of similarity transformations is used to reduce the governing partial differential Eq. (1) – (3) to a set of ordinary differential equations. The similarity equations are

$$\eta=\frac{r^2-R^2}{2R}\sqrt{\frac{b}{v_f L}}, \psi=\sqrt{\frac{bv_f}{L}}xRf(\eta), T=(T_w(x)-T_0)\theta(\eta)+T_\infty(x), \tag{6}$$

where $u=\frac{1}{r}\frac{\partial\psi}{\partial r}$ and $v=-\frac{1}{r}\frac{\partial\psi}{\partial x}$ which obeys Eq. (1). Therefore, the new transformed similarity differential equations with the coupled conditions are given by

$$\frac{\frac{\mu_{hnf}}{\mu_f}}{\frac{\rho_{hnf}}{\rho_f}}[(1+2\gamma\eta)f'''+2\gamma f'']=f'^2-ff''-1-A_1\lambda\theta, \tag{7}$$

$$\frac{1}{Pr}\frac{{k_{hnf}}/{k_f}}{{(\rho C_p)_{hnf}}/{(\rho C_p)_f}}[(1+2\gamma\eta)\theta''+2\gamma\theta']=(\theta+\delta)f'-f\theta', \tag{8}$$

$$f(\eta)=S, f'(\eta)=\varepsilon, \theta(\eta)=1-\delta \text{ at } \eta=0,$$
$$f'(\eta)\to 1, \theta(\eta)\to 0 \text{ as } \eta\to\infty, \tag{9}$$

And

$$A_1 = \frac{(1-\phi_2)\left[(1-\phi_1)\rho_f+\phi_1\frac{(\rho\beta_T)_{s1}}{(\beta_T)_f}\right]+\phi_2\frac{(\rho\beta_T)_{s2}}{(\beta_T)_f}}{(1-\phi_2)[(1-\phi_1)\rho_f+\phi_1\rho_{s1}]+\phi_2\rho_{s2}}. \quad (10)$$

The curvature of the cylindrical surface, thermal convection and thermal stratification parameters are in the form of

$$\gamma = \sqrt{L\nu_f/bR^2}, \quad \lambda = \frac{Gr_x}{\mathrm{Re}_x^{\,2}} = \frac{g(\beta_T)_f(T_w-T_0)x^3/\nu_f^{\,2}}{\left(bx^2/L\nu_f\right)^2}, \quad \delta = B/A, \quad (11)$$

accordingly. In addition, $S > 0$ stands for suction parameter and $S < 0$ for injection parameter. $s1$ and $s2$ represent the first and second type of the nanoparticles while ϕ_1 and ϕ_2 are the first and second nanoparticles solid volume fractions, proportionately. $\varepsilon = \frac{a}{b}$ stands for the velocity ratio parameter and for case $\gamma > 0$ (cylinder), $\varepsilon > 0$ corresponds to the stretching flow case whereas $\varepsilon < 0$ corresponds to the shrinking flow case. The present problem is reduced to the stretching/shrinking flat surface if the value of γ is zero. In addition, $\lambda < 0$, $\lambda = 0$ and $\lambda > 0$ imply the opposing, forced convective and assisting flow, respectively.

Table 2 elucidates the values of the thermophysical properties (ρ, C_p, k, β_T) between the nanoparticles (copper, alumina) and regular fluid (water).

Table 1
The thermophysical properties between hybrid and traditional nanofluids (see Devi and Devi [17], Rostami *et al.,* [31] and Das and Jana [45])

Properties	Hybrid Nanofluid	Traditional Nanofluid
Density	$\rho_{hnf} = (1-\phi_2)\left[(1-\phi_1)\rho_f + \phi_1\rho_{s1}\right] + \phi_2\rho_{s2}$	$\rho_{nf} = (1-\phi)\rho_f + \phi\rho_s$
Heat Capacity	$(\rho C_p)_{hnf} = (1-\phi_2)\left[(1-\phi_1)(\rho c_p)_f + \phi_1(\rho c_p)_{s1}\right] + \phi_2(\rho c_p)_{s2}$	$(\rho C_p)_{nf} = (1-\phi)(\rho c_p)_f + \phi(\rho c_p)_s$
Dynamic Viscocity	$\frac{\mu_{hnf}}{\mu_f} = \frac{1}{(1-\phi_1)^{2.5}(1-\phi_2)^{2.5}}$	$\frac{\mu_{nf}}{\mu_f} = \frac{1}{(1-\phi_1)^{2.5}}$
Thermal Conductivity	$k_{hnf} = \left[\frac{k_{s2}+2k_{bf}-2\phi_2(k_{bf}-k_{s2})}{k_{s2}+2k_{bf}+\phi_2(k_{bf}-k_{s2})}\right]k_{bf}$ where $k_{bf} = \left[\frac{k_{s1}+2k_f-2\phi_1(k_f-k_{s1})}{k_{s1}+2k_f+\phi_1(k_f-k_{s1})}\right]k_f$	$k_{nf} = \left[\frac{k_s+2k_f-2\phi(k_f-k_s)}{k_s+2k_f+\phi(k_f-k_s)}\right]k_f$
Thermal Expansion	$(\rho\beta_T)_{hnf} = (1-\phi_2)\left[(1-\phi_1)(\rho\beta_T)_f + \phi_1(\rho\beta_T)_{s1}\right] + \phi_2(\rho\beta_T)_{s2}$	$(\rho\beta_T)_{nf} = (1-\phi)(\rho\beta_T)_f + \phi(\rho\beta_T)_s$

Table 2
Thermophysical properties of the alumina, copper and water (see Rostami *et al.,* [31], Das and Jana [45] and Oztop and Abu-Nada [46])

Physical properties	$\rho\left(\frac{\mathrm{kg}}{m^3}\right)$	$C_p\left(\frac{J}{\mathrm{kgK}}\right)$	$k\left(\frac{W}{\mathrm{mK}}\right)$	$\beta_T(K^{-1})$
Alumina	3970	765	40	0.85×10^{-5}
Copper	8933	385	400	1.67×10^{-5}
Water	997.1	4179	0.6130	21×10^{-5}

The main physical interests of the study are the skin friction coefficient C_f and the local Nusselt number Nu_x which are generally in the form of

$$C_f = \frac{\tau_w}{\rho_f u_e^2}, \qquad Nu_x = \frac{x q_w}{k_f(T_w(x)-T_0)}, \tag{12}$$

where τ_w is the surface shear stress and q_w is the surface heat flux

$$\tau_w = \mu_{hnf}\left(\frac{\partial u}{\partial r}\right)_{r=R}, \qquad q_w = -k_{hnf}\left(\frac{\partial T}{\partial r}\right)_{r=R}. \tag{13}$$

Using Eq. (6), (12) and (13), the reduced skin friction coefficient and reduced local Nusselt number are given by

$$Re_x^{1/2} C_f = \frac{\mu_{hnf}}{\mu_f} f''(0), \qquad Re_x^{-1/2} Nu_x = -\frac{k_{hnf}}{k_f}\theta'(0), \tag{14}$$

where $Re_x = u_e(x)x/\nu_f$ is the local Reynolds number.

3. Temporal Stability Analysis

Generally, zero, unique or multiple solutions are possible in a boundary layer flow problem. For the case of non-unique or multiple solutions, the first (upper branch) solution is assigned to the solution which initially satisfies the far field boundary condition. In most problem, the stability analysis has proved that the first solution is the physical and stable solution. However, there also exist a problem where lower branch solution is stable as reported by Weidman *et al.,* [47]. Hence, it is important to execute the stability analysis and validate the reliability of the solution(s). The solution is not physical (real) if an initial growth of disturbance appears in the solution. The disturbance (perturbation) may exponentially decay or increase with time. This is the reason for considering an unsteady problem in the stability formulation. Following Merkin [48], an unsteady form of Eq. (2) and (3) is considered which are

$$\frac{\partial u}{\partial t} + u\frac{\partial u}{\partial x} + v\frac{\partial u}{\partial r} = u_e\frac{du_e}{dx} + \frac{\mu_{hnf}}{\rho_{hnf}}\left(\frac{\partial^2 u}{\partial r^2} + \frac{1}{r}\frac{\partial u}{\partial r}\right) + \frac{(\rho\beta_T)_{hnf} g(T-T_\infty)}{\rho_{hnf}}, \tag{15}$$

$$\frac{\partial T}{\partial t} + u\frac{\partial T}{\partial x} + v\frac{\partial T}{\partial r} = \left(\frac{k}{\rho c_p}\right)_{hnf}\left(\frac{\partial^2 T}{\partial r^2} + \frac{1}{r}\frac{\partial T}{\partial r}\right), \tag{16}$$

and the relevant similarity transformation is given by

$$\eta = \frac{r^2-R^2}{2R}\sqrt{\frac{b}{\nu_f L}}, \psi = \sqrt{\frac{b\nu_f}{L}} xRf(\eta,\tau), T = (T_w(x)-T_0)\theta(\eta,\tau) + T_\infty(x), \tag{17}$$

where $\tau = \frac{b}{L}t$. Using Eq. (15), Eqs. (13) and (14) can be rewritten as

$$\frac{\frac{\mu_{hnf}}{\mu_f}}{\frac{\rho_{hnf}}{\rho_f}}\left[(1+2\gamma\eta)\frac{\partial^3 f}{\partial\eta^3} + 2\gamma\frac{\partial^2 f}{\partial\eta^2}\right] + 1 + f\frac{\partial^2 f}{\partial\eta^2} - \left(\frac{\partial f}{\partial\eta}\right)^2 + A_1\lambda\theta - \frac{\partial^2 f}{\partial\eta\partial\tau} = 0, \tag{18}$$

$$\frac{1}{Pr}\frac{{k_{hnf}}/{k_f}}{{(\rho C_p)_{hnf}}/{(\rho C_p)_f}}\left[(1+2\gamma\eta)\frac{\partial^2\theta}{\partial\eta^2}+2\gamma\frac{\partial\theta}{\partial\eta}\right]+f\frac{\partial\theta}{\partial\eta}-\frac{\partial f}{\partial\eta}(\theta+\delta)-\frac{\partial\theta}{\partial\tau}=0, \tag{19}$$

with the transformed conditions

$$f(0,\tau)=S,\ \frac{\partial f}{\partial\eta}(0,\tau)=\varepsilon,\ \theta(0,\tau)=1-\delta,$$
$$\frac{\partial f}{\partial\eta}(\eta,\tau)\to 1,\ \theta(\eta,\tau)\to 0 \text{ as } \eta\to\infty. \tag{20}$$

According to Weidman *et al.,* [49], the following perturbation equations (see Eq. (19)) are introduced to investigate the stability of the similarity solutions $f(\eta)=f_0(\eta)$ and $\theta(\eta)=\theta_0(\eta)$. An unknown eigenvalue σ is used in the formulation whereas $F(\eta)$ and $G(\eta)$ are a small relative to $f_0(\eta)$ and $\theta_0(\eta)$, correspondingly. However, the solutions' stability are tested by choosing the smallest eigenvalue σ_1 among the computed σ.

$$f(\eta,\tau)=f_0(\eta)+e^{-\sigma\tau}F(\eta),$$
$$\theta(\eta,\tau)=\theta_0(\eta)+e^{-\sigma\tau}G(\eta), \tag{21}$$

Hence, by employing Eq. (19) into Eqs. (16)-(18), the following linearized eigenvalue problem is attained such that

$$\frac{\frac{\mu_{hnf}}{\mu_f}}{\frac{\rho_{hnf}}{\rho_f}}[(1+2\gamma\eta)F'''+2\gamma F'']+f_0F''-(2f_0{}'-\sigma)F'+f_0{}''F+A_1\lambda G=0, \tag{22}$$

$$\frac{1}{Pr}\frac{{k_{hnf}}/{k_f}}{{(\rho C_p)_{hnf}}/{(\rho C_p)_f}}[(1+2\gamma\eta)G''+2\gamma G']+F\theta_0{}'+f_0G'-(\theta_0+\delta)F'-(f_0{}'-\sigma)G=0, \tag{23}$$

$$F'(0)=F(0)=G(0)=0,$$
$$F'(\eta)\to 0,\ G(\eta)\to 0 \text{ as } \eta\to\infty. \tag{24}$$

The smallest eigenvalue σ_1 will determine the stability of the similarity solutions such that positive value of σ_1 implies that the solution is real or stable. In contrast, negative σ_1 indicates that the steady solution is unstable. Hence, to find the possible range of the smallest eigenvalue σ_1, Eqs. (22)-(24) are computed using the bvp4c solver. However, a modification for Eq. (24) is needed so that the bvp4c code can be successfully executed. Following Harris *et al.,* [50], $F'(\infty)$ in Eq. (24) is relaxed and substituted with a new condition $F''(0)=1$.

4. Results and Discussion

The similarity solutions of the ordinary differential equations (see Eqs. (7) and (8)) coupled with the boundary conditions (9) are attained by using the bvp4c solver in the Matlab software. The combination of appropriate guess value, boundary layer thickness η_∞ and the value of the control parameters may lead to the existence of the unique or multiple solutions within the specified

accuracy. The objectives of the present work are (a) to study the effect of parameters namely suction S, the surface curvature γ, thermal buoyancy parameter λ and copper nanoparticles volume fraction ϕ_2 when the stratified fluid is considered, and (b) to identify all the potential solutions arise from the governing model. In the present study, $\eta_\infty = 15$ and alumina nanoparticles volume fraction $\phi_2 = 0.1$ are fixed whereas $Pr = 6.2$ is used to represent the water (viscous fluid) as the base fluid (see Oztop and Abu-Nada [46]). A comparison between present data and previously published literatures (see Table 3) are conducted for the validation of the present model. Omar *et al.,* [43] solved the stagnation point flow of Cu-water nanofluid over a stretching/shrinking cylinder whereas Bachok *et al.,* [51] studied the stagnation point flow of nanofluid over a stretching/shrinking sheet. Both literatures adopted shooting method for the numerical computation. It is apparent from Table 3 that the comparison values of $f''(0)$ between present method and the existing literatures are in a good agreement, hence the authors are confident to use the model in the present work.

Table 3
The comparison values of $f''(0)$for different stretching/shrinking parameter (ε) and curvature parameter (γ) when $\phi_2 = 0.1, \phi_1 = 0, Pr = 6.2$ and $\delta = \lambda = S = 0$

ε	Present		Omar *et al.,* [43] (shooting method)		Bachok *et al.,* [51] (shooting method)	
	$\gamma = 0$	$\gamma = 0.4$	$\gamma = 0$	$\gamma = 0.4$	$\gamma = 0$	$\gamma = 0.4$
2	-2.217106	-2.396084	-2.217106	-2.396084	-2.217106	-
1	0	0	0	0	0	-
0.5	0.837940	0.935394	0.837940	0.935394	0.837940	-
0	1.447977	1.653867	1.447977	1.653867	1.447977	-
-0.5	1.757032	2.096118	1.757022	2.096118	1.757032	-
-1.15	1.271347	2.003737	1.271347	2.003737	1.271347	-
	[0.137095]	[-0.131198]	[0.137095]	[-0.131198]	[0.137095]	
-1.2	1.095419	1.939265	1.095419	1.939265	1.095419	-
	[0.274479]	[-0.101872]	[0.274479]	[-0.101872]	[0.274479]	
-1.2465	0.686382	1.865189	0.686380	1.865189	0.686379	-
	[0.651157]	[-0.052290]	[0.651160]	[-0.052290]	[0.651161]	

The diversity of $Re_x^{\frac{1}{2}}C_f$ and $Re_x^{\frac{-1}{2}}Nu_x$ towards S with the enhancement of the curvature parameter γ and copper solid volume fractions ϕ_2 are manifested in Figures 2 and 3, respectively. The application of suitable wall mass suction parameter $(S > 0)$ can generate the dual similarity solutions in the present work as interpreted in Figures 2 and 3. Nevertheless, if the cylinder is impermeable $(S = 0)$ or injection parameter $(S < 0)$ is applied, no similarity solutions (unique or dual) can be obtained. Figure 2 shows that less value of suction parameter S (less magnitude) is needed if the curvature parameter increases. However, in the present work, the authors only test the value of γ within the range of $0 \leq \gamma \leq 0.1$ and if $\gamma > 0.1$, the result may be different. For each value of S, both skin friction coefficient and heat transfer rate of shrinking cylinder $(\gamma = 0.1)$ is greater as compared to the shrinking flat surface $(\gamma = 0)$.

Figure 3 displays the $Re_x^{\frac{1}{2}}C_f$ and $Re_x^{\frac{-1}{2}}Nu_x$ when ϕ_2 is enhanced. It shows that both $Re_x^{\frac{1}{2}}C_f$ and $Re_x^{\frac{-1}{2}}Nu_x$ intensify with the increment of ϕ_2. However, the result of heat transfer rate may differ if $S > 1$ is considered. It is clear in Figure 3(b) that as $S \to 1$, the heat transfer rate only slightly increases when ϕ_2 is increased. Figure 4 portrays the variations of $Re_x^{\frac{1}{2}}C_f$ and $Re_x^{\frac{-1}{2}}Nu_x$ towards the mixed convection parameter λ for different values of γ. The dual solutions are possible in the opposing flow region $(\lambda < 0)$ and assisting flow region $(\lambda > 0)$ while only unique solution is attained

for the forced convective flow ($\lambda = 0$). However, it can be seen that in the assisting flow region, the second solution only can be achieved for a limited value of positive λ. Further investigation is required to study the parameters which can maintain the existence of the second solution in the assisting flow region. Additionally, the second solution for $Re_x^{\frac{-1}{2}} Nu_x$ becomes unbounded as $\lambda \to 0$ from left ($\lambda \to 0^-$) and right ($\lambda \to 0^+$). Figure 4 also reveals that the cylindrical surface ($\gamma > 0$) also can increase the existence range of the similarity solutions to Eqs. (7)-(9) and consequently, delays the boundary layer separation.

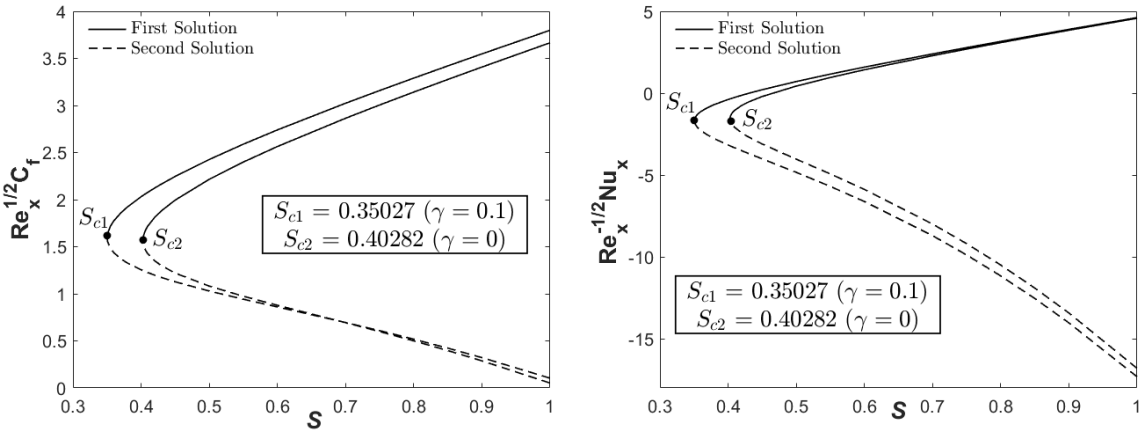

(a) (b)

Fig. 2. (a) $Re_x^{\frac{1}{2}} C_f$ (b) $Re_x^{\frac{-1}{2}} Nu_x$ towards S for shrinking flat surface ($\gamma = 0$) and shrinking cylinder ($\gamma = 0.1$)when $\varepsilon = \lambda = -1$ and $\phi_2 = \delta = 0.005$

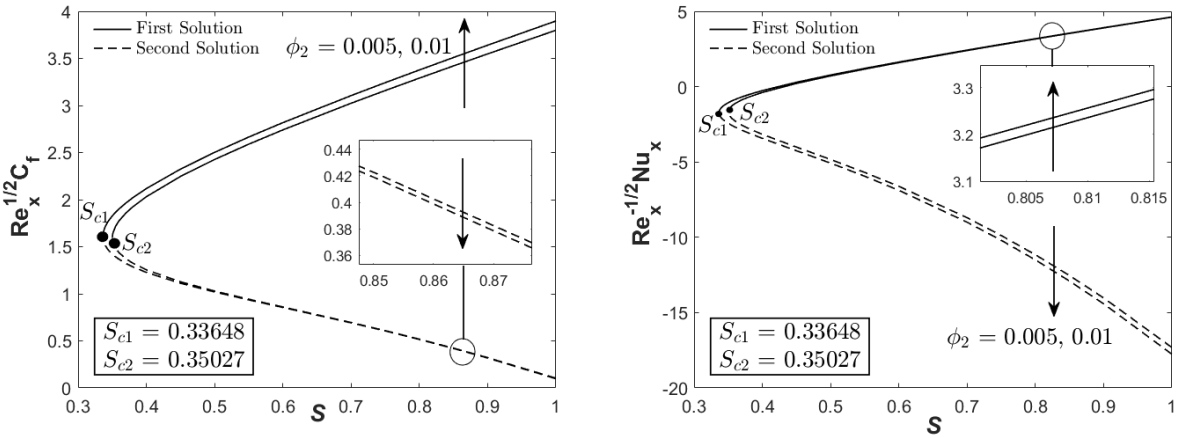

(a) (b)

Fig. 3. (a) $Re_x^{\frac{1}{2}} C_f$ (b) $Re_x^{\frac{-1}{2}} Nu_x$ towards S for different ϕ_2 when $\gamma = 0.1$, $\varepsilon = \lambda = -1$ and $\delta = 0.005$

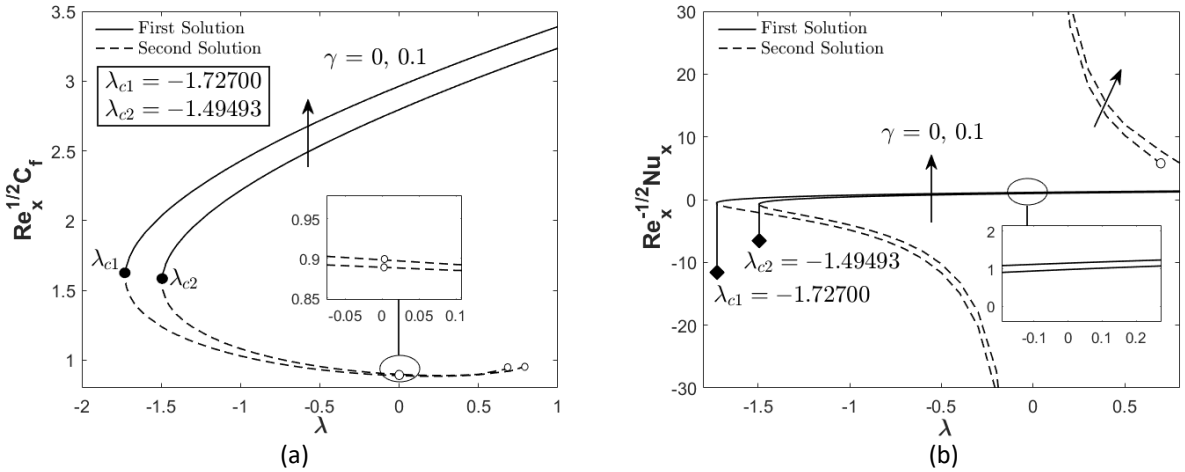

Fig. 4. (a) $Re_x^{\frac{1}{2}}C_f$ (b) $Re_x^{\frac{-1}{2}}Nu_x$ towards λ for various γ when $S = 0.5$, $\varepsilon = -1$ and $\phi_2 = \delta = 0.005$

Figure 5 presents the comparison of heat transfer rate between traditional and hybrid nanofluids with disparate volumetric concentration. The heat transfer rate of alumina-water nanofluids are the lowest as compared to Cu-water and hybrid Cu-Al_2O_3/water nanofluids. However, the combination of alumina and copper nanoparticles with the suitable nanoparticles volumetric concentrations can create a hybrid nanofluid with greater heat transfer rate. The velocity and temperature profiles for shrinking cylinder case ($\varepsilon < 0$), stretching cylinder case ($\varepsilon > 0$) and static cylinder case ($\varepsilon = 0$) are exhibited in Figure 6. The fluid velocity decreases when the velocity ratio parameter decrease whereas a contradictory result is obtained for the temperature profile. Otherwise, the second solution shows a different result as compared to the first solution. Figures 7 and 8 display the velocity and temperature profiles for various values of copper solid volume fraction and curvature parameters. A slight increment of velocity profile is noticed in Figure 7 whereas the temperature profile shows an adverse result. The nanoparticles physically is added to dispense energy in the heat form (see Devi and Devi [17]). Under assisting buoyancy environment, an upsurge of nanoparticles volumetric concentration increase both velocity and temperature profiles as reported by Khashi'ie *et al.,* [52]. However, the present work reveals different result where the temperature profile reduces with an increase of ϕ_2 as a result of opposing buoyancy ($\lambda = -1$) and shrinking cylinder ($\varepsilon = -1, \gamma = 0.1$). Figure 8 shows that the velocity and temperature profiles are different when $\eta < 1$ and $\eta > 1$ (boundary layer thickens) with an increase in the curvature parameter. Far from the surface, the fluid velocity starts decreasing whereas the temperature inflates with an addition of the curvature parameter.

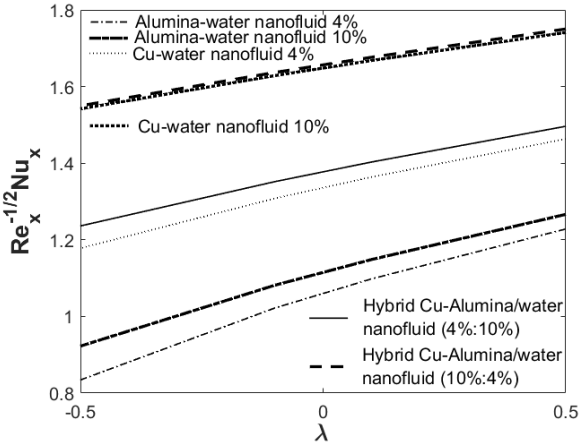

Fig. 5. $Re_x^{\frac{-1}{2}}Nu_x$ towards λ for single and hybrid nanofluids with different concentration when $S = 0.5$, $\varepsilon = -1$ and $\delta = 0.005$

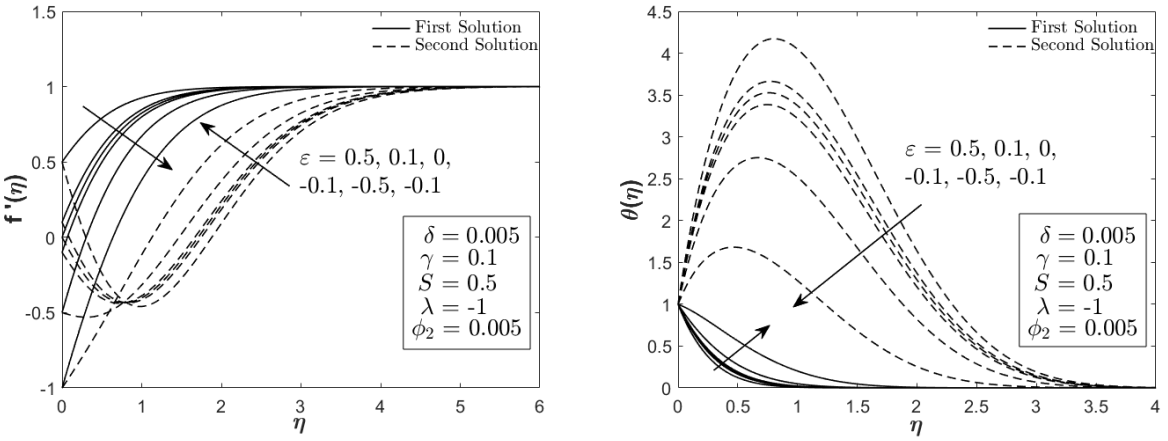

(a) (b)

Fig. 6. (a) Velocity (b) Temperature profiles for various values of velocity ratio parameter

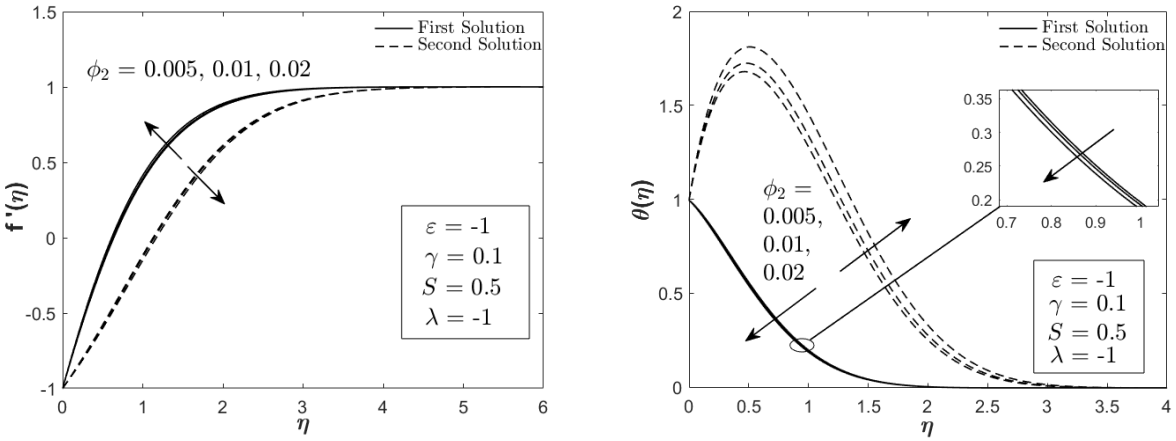

(a) (b)

Fig. 7. (a) Velocity (b) Temperature profiles for various values of copper nanoparticles volume fraction when $\delta = 0.005$

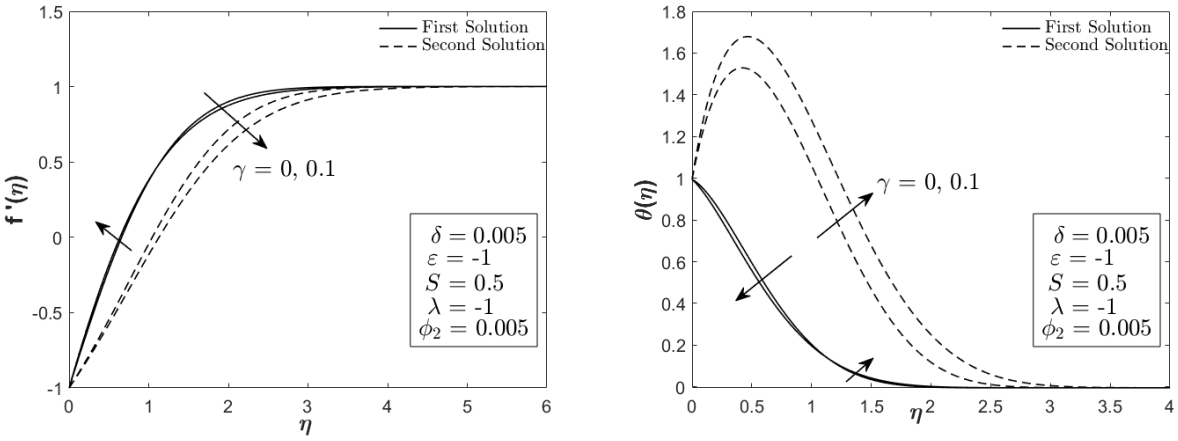

Fig. 8. (a) Velocity (b) Temperature profiles for various values of curvature parameter

The stability of similarity solutions are determined by finding the smallest eigenvalue σ_1. Thus, Eq. (22)-(24) with the new boundary condition are solved using the efficient bvp4c solver (code c and d). It is apparent from Figure 9 that the first solution has positive σ_1 while reverse results for the second solution. Figure 9 also depicts that σ_1 for both similarity solutions approach to 0 as $\lambda \to \lambda_c$ which justifies the fact that at $\lambda = \lambda_c$, the value of σ_1 is zero. Hence, it is provable that the first solution is more realistic and virtual than the second solution.

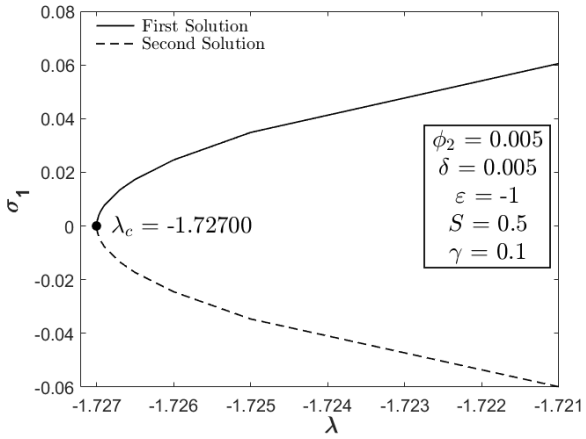

Fig. 9. The smallest eigenvalue σ_1 towards λ for both first and second solutions

5. Conclusions

The present work deals with the numerical solution of stagnation point flow and heat transfer of a hybrid nanofluid over a vertical permeable stretching/shrinking cylinder. Thermal stratification process is considered as a result of a variable (linear stratified) ambient temperature while the wall temperature is also in a variable form to illustrate the mixed convection phenomenon. The present model in partial differential equations are converted to a nonlinear system of ordinary (similarity) differential equations using the similarity variable and further, computed using the boundary value problem solver (bvp4c) in the Matlab software. The conclusions are

- The similarity solutions (first and second) are attained for the shrinking cylinder case when low magnitude of suction parameter is imposed. No possible solution(s) if the cylinder is impermeable or injection parameter is applied.
- The higher values of curvature γ and copper nanoparticles volume fractions ϕ_2 parameters may inflate the reduced skin friction coefficient and local Nusselt number within the specific value of suction parameter.
- The first similarity solution exists for all values of the buoyancy parameter up to the critical value whereas the second similarity solution is impossible for the forced convective flow and higher magnitude of assisting flow.
- The execution of stability analysis proves the reliability of the first solution.
- The present work may contribute idea to the other researchers from various background (mathematics, mechanical, physics) on how to control (increase/decrease) the heat transfer rate by manipulating the parameters or the possibilities of gaining non-unique solutions in the computation.
- The present results only applicable to the combination of copper and alumina nanoparticles only. However, other researchers may extend the study using other hybrid nanofluids or physical parameters to achieve the desired outcome.

Acknowledgement
This project was funded by Universiti Putra Malaysia (GP-IPM/2018/9619000). The support from Ministry of Education (Malaysia) and Universiti Teknikal Malaysia Melaka (UTEM-SLAB scholarship) also highly appreciated.

References

[1] Sidik, Nor Azwadi Che, Isa Muhammad Adamu, Muhammad Mahmud Jamil, G. H. R. Kefayati, Rizalman Mamat, and G. Najafi. "Recent progress on hybrid nanofluids in heat transfer applications: a comprehensive review." *International Communications in Heat and Mass Transfer* 78 (2016): 68-79.
[2] Shah, Tayyab Raza, and Hafiz Muhammad Ali. "Applications of hybrid nanofluids in solar energy, practical limitations and challenges: a critical review." *Solar Energy* 183 (2019): 173-203.
[3] Xian, Hong Wei, Nor Azwadi Che Sidik, Siti Rahmah Aid, Tan Lit Ken, and Yutaka Asako. "Review on preparation techniques, properties and performance of hybrid nanofluid in recent engineering applications." *Journal of Advanced Research in Fluid Mechanics and Thermal Sciences* 45, no. 1 (2018): 1-13.
[4] Kumar, D. Dhinesh, and A. Valan Arasu. "A comprehensive review of preparation, characterization, properties and stability of hybrid nanofluids." *Renewable and Sustainable Energy Reviews* 81 (2018): 1669-1689.
[5] Esfe, Mohammad Hemmat, Mahmoud Kiannejad Amiri, and Ali Alirezaie. "Thermal conductivity of a hybrid nanofluid." *Journal of Thermal Analysis and Calorimetry* 134, no. 2 (2018): 1113-1122.
[6] Sajid, Muhammad Usman, and Hafiz Muhammad Ali. "Thermal conductivity of hybrid nanofluids: a critical review." *International Journal of Heat and Mass Transfer* 126 (2018): 211-234.
[7] Gupta, Munish, Vinay Singh, Satish Kumar, Sandeep Kumar, Neeraj Dilbaghi, and Zafar Said. "Up to date review on the synthesis and thermophysical properties of hybrid nanofluids." *Journal of cleaner production* 190 (2018): 169-192.
[8] Huminic, Gabriela, and Angel Huminic. "Hybrid nanofluids for heat transfer applications–a state-of-the-art review." *International Journal of Heat and Mass Transfer* 125 (2018): 82-103.
[9] Buongiorno, Jacopo. "Convective transport in nanofluids." *Journal of Heat Transfer* 128, no.3 (2006): 240-250.
[10] Tiwari, Raj Kamal, and Manab Kumar Das. "Heat transfer augmentation in a two-sided lid-driven differentially heated square cavity utilizing nanofluids." *International Journal of heat and Mass transfer* 50, no. 9-10 (2007): 2002-2018.
[11] Khashi'ie, Najiyah Safwa, Norihan Md Arifin, Ezad Hafidz Hafidzuddin, Nadihah Wahi, and Mohd Rijal Ilias. "Magnetohydrodynamics (MHD) Flow and Heat Transfer of a Doubly Stratified Nanofluid Using Cattaneo-Christov Model." *Universal Journal of Mechanical Engineering* 7, no. 4 (2019):206-214.

[12] Khashi'ie, Najiyah Safwa, Norihan Md Arifin, Ezad Hafidz Hafidzuddin, and Nadihah Wahi. "Dual stratified nanofluid flow past a permeable shrinking/stretching sheet using a non-Fourier energy model." *Applied Sciences* 9, no. 10 (2019): 2124.
[13] Reza-E-Rabbi, Sk, Sarder Firoz Ahmmed, S. M. Arifuzzaman, Tanmoy Sarkar, and Md Shakhaoath Khan. "Computational modelling of multiphase fluid flow behaviour over a stretching sheet in the presence of nanoparticles." *Engineering Science and Technology, an International Journal* (2019).
[14] Reza-E-Rabbi, Sk, S. M. Arifuzzaman, Tanmoy Sarkar, Md Shakhaoath Khan, and Sarder Firoz Ahmmed. "Explicit finite difference analysis of an unsteady MHD flow of a chemically reacting Casson fluid past a stretching sheet with Brownian motion and thermophoresis effects." *Journal of King Saud University-Science* 32, no. 1 (2020):690-701.
[15] Rana, B. M. J., S. M. Arifuzzaman, Sk Reza-E-Rabbi, S. F. Ahmed, and Md Shakhaoath Khan. "Energy and magnetic flow analysis of Williamson micropolar nanofluid through stretching sheet." *International Journal of Heat and Technology* 37, no. 2 (2019): 487-496.
[16] Khan, Md, Ifsana Karim, Md Rahman, S. M. Arifuzzaman, and Pronab Biswas. "Williamson fluid flow behaviour of MHD convective-radiative Cattaneo–Christov heat flux type over a linearly stretched-surface with heat generation and thermal-diffusion." *Frontiers in Heat and Mass Transfer (FHMT)* 9, no. 1 (2017).
[17] Devi, SP Anjali, and S. Suriya Uma Devi. "Numerical investigation of hydromagnetic hybrid Cu–Al2O3/water nanofluid flow over a permeable stretching sheet with suction." *International Journal of Nonlinear Sciences and Numerical Simulation* 17, no. 5 (2016): 249-257.
[18] Hiemenz, Karl. "Die Grenzschicht an einem in den gleichformigen Flussigkeitsstrom eingetauchten geraden Kreiszylinder." *Dinglers Polytech J* 326, (1911): 321-324.
[19] Homann, Fritz. "Der Einfluss grosser Zähigkeit bei der Strömung um den Zylinder und um die Kugel." *ZAMM-Journal of Applied Mathematics and Mechanics/Zeitschrift für Angewandte Mathematik und Mechanik* 16, no. 3 (1936): 153-164.
[20] TC, Chiam. "Stagnation-point flow towards a stretching plate." *Journal of the physical society of Japan* 63, no. 6 (1994): 2443-2444.
[21] Wang, C.Y. "Stagnation flow towards a shrinking sheet." *International Journal of Non-Linear Mechanics* 43, no. 5 (2008): 377-382.
[22] Awaludin, I. S., P. D. Weidman, and Anuar Ishak. "Stability analysis of stagnation-point flow over a stretching/shrinking sheet." *AIP Advances* 6, no. 4 (2016): p.045308.
[23] Khashi'ie, Najiyah Safwa, Norihan Md Arifin, Mohammad Mehdi Rashidi, Ezad Hafidz Hafidzuddin, and Nadihah Wahi. "Magnetohydrodynamics (MHD) stagnation point flow past a shrinking/stretching surface with double stratification effect in a porous medium." *Journal of Thermal Analysis and Calorimetry* (2019): 1-14.
[24] Nasir, Nor Ain Azeany Mohd, Anuar Ishak, and Ioan Pop. "Stagnation-Point Flow Past a Permeable Stretching/Shrinking Sheet." *Advanced Science Letters* 23, no. 11 (2017): 11040-11043.
[25] Nasir, Nor Ain Azeany Mohd, Anuar Ishak, and Ioan Pop. "Stagnation-point flow and heat transfer past a permeable quadratically stretching/shrinking sheet." *Chinese Journal of Physics* 55, no. 5 (2017): 2081-2091.
[26] Nasir, Nor Ain Azeany Mohd, Anuar Ishak, and Ioan Pop. "Stagnation point flow and heat transfer past a permeable stretching/shrinking Riga plate with velocity slip and radiation effects." *Journal of Zhejiang University-SCIENCE A* 20, no. 4 (2019): 290-299.
[27] Kamal, Fatinnabila, Khairy Zaimi, Anuar Ishak, and Ioan Pop. "Stability analysis on the stagnation-point flow and heat transfer over a permeable stretching/shrinking sheet with heat source effect." *International Journal of Numerical Methods for Heat & Fluid Flow* 28, no. 11 (2018):2650-2663.
[28] Kamal, Fatin Nabila., Khairy Zaimi, Anuar Ishak, and Ioan Pop. "Stability analysis of MHD stagnation-point flow towards a permeable stretching/shrinking sheet in a nanofluid with chemical reactions effect." *Sains Malaysiana* 48, no. 1 (2019): 243-250.
[29] Khashi'ie, Najiyah Safwa, Norihan Md Arifin, Roslinda Nazar, Ezad Hafidz Hafidzuddin, Nadihah Wahi, and Ioan Pop. "A stability analysis for magnetohydrodynamics stagnation point flow with zero nanoparticles flux condition and anisotropic slip." *Energies* 12, no. 7 (2019): 1268.
[30] Khashi'ie, Najiyah Safwa, Norihan Md Arifin, Ioan Pop, Roslinda Nazar, Ezad Hafidz Hafidzuddin, and Nadihah Wahi. "Non-axisymmetric Homann stagnation point flow and heat transfer past a stretching/shrinking sheet using hybrid nanofluid." *International Journal of Numerical Methods for Heat & Fluid Flow* (2020).
[31] Rostami, Mohammadreza Nademi, Saeed Dinarvand, and Ioan Pop. "Dual solutions for mixed convective stagnation-point flow of an aqueous silica–alumina hybrid nanofluid." *Chinese Journal of Physics* 56, no. 5 (2018): 2465-2478.
[32] Khashi'ie, Najiyah Safwa, Norihan Md Arifin, Roslinda Nazar, Ezad Hafidz Hafidzuddin, Nadihah Wahi, and Ioan Pop. "Magnetohydrodynamics (MHD) Axisymmetric Flow and Heat Transfer of a Hybrid Nanofluid past a Radially Permeable Stretching/Shrinking Sheet with Joule Heating." *Chinese Journal of Physics* (2019).

[33] Waini, I., A. Ishak, and I. Pop. "MHD flow and heat transfer of a hybrid nanofluid past a permeable stretching/shrinking wedge." *Applied Mathematics and Mechanics* (2020): 1-14.
[34] Wang, C.Y. "Fluid flow due to a stretching cylinder." *The Physics of fluids* 31, no. 3 (1988): 466-468.
[35] Ishak, Anuar Mohd, and Roslinda Mohd Nazar. "Laminar boundary layer flow along a stretching cylinder." *European Journal of Scientific Research* 36, no. 1 (2009): 22-29.
[36] Poply, Vikas, Phool Singh, and A. K. Yadav. "Stability analysis of MHD outer velocity flow on a stretching cylinder." *Alexandria engineering journal* 57, no. 3 (2018): 2077-2083.
[37] Vinita, V., and Vikas Poply. "Impact of outer velocity MHD slip flow and heat transfer of nanofluid past a stretching cylinder." *Materials Today: Proceedings* (2019).
[38] Ishak, A. "Mixed convection boundary layer flow over a vertical cylinder with prescribed surface heat flux." *Journal of Physics A: Mathematical and Theoretical* 42, no. 19 (2009): p.195501.
[39] Bachok, Norfifah, and Anuar Mohd Ishak. "Mixed convection boundary layer flow over a permeable vertical cylinder with prescribed surface heat flux." *European Journal of Scientific Research* 34, no. 1 (2009): 46-54.
[40] Arifuzzaman, S. M., Md Shakhaoath Khan, Abdullah Al-Mamun, Sk Reza-E-Rabbi, Pronab Biswas, and Ifsana Karim. "Hydrodynamic stability and heat and mass transfer flow analysis of MHD radiative fourth-grade fluid through porous plate with chemical reaction." *Journal of King Saud University-Science* 31, no. 4 (2019): 1388-1398.
[41] Khashi'ie, Najiyah Safwa, Norihan Md Arifin, Ezad Hafidz Hafidzuddin, and Nadihah Wahi. "Thermally Stratified Flow of Cu-Al2O3/water Hybrid Nanofluid past a Permeable Stretching/Shrinking Circular Cylinder." *Journal of Advanced Research in Fluid Mechanics and Thermal Sciences* 63, no.1 (2019): 154-163.
[42] Najib, N., Bachok, N., Arifin, N.M. and Ishak, A. "Stagnation point flow and mass transfer with chemical reaction past a stretching/shrinking cylinder." *Scientific reports* 4, (2014): 4178.
[43] Omar, Noor Syamimi, Norfifah Bachok, and Norihan Md Arifin. "Stagnation point flow over a stretching or shrinking cylinder in a copper-water nanofluid." *Indian Journal of Science and Technology* 8, (2015): 1-7.
[44] Nadeem, S., Nadeem Abbas, and A. U. Khan. "Characteristics of three dimensional stagnation point flow of Hybrid nanofluid past a circular cylinder." *Results in physics* 8, (2018): 829-835.
[45] Das, S., and R. N. Jana. "Natural convective magneto-nanofluid flow and radiative heat transfer past a moving vertical plate." *Alexandria Engineering Journal* 54, no. 1 (2015): 55-64.
[46] Oztop, Hakan F., and Eiyad Abu-Nada. "Numerical study of natural convection in partially heated rectangular enclosures filled with nanofluids." *International journal of heat and fluid flow* 29, no. 5 (2008): 1326-1336.
[47] Weidman, P. D., A. M. J. Davis, and D. G. Kubitschek. "Crocco variable formulation for uniform shear flow over a stretching surface with transpiration: multiple solutions and stability." *Zeitschrift für angewandte Mathematik und Physik* 59, no. 2 (2008): 313-332.
[48] Merkin, J.H. "On dual solutions occurring in mixed convection in a porous medium." *Journal of engineering Mathematics* 20, no. 2 (1986): 171-179.
[49] Weidman, P. D., D. G. Kubitschek, and A. M. J. Davis. "The effect of transpiration on self-similar boundary layer flow over moving surfaces." *International journal of engineering science* 44, no. 11-12 (2006): 730-737.
[50] Harris, S. D., D. B. Ingham, and I. Pop. "Mixed convection boundary-layer flow near the stagnation point on a vertical surface in a porous medium: Brinkman model with slip." *Transport in Porous Media* 77, no. 2 (2009): 267-285.
[51] Bachok, Norfifah, Anuar Ishak, and Ioan Pop. "Stagnation-point flow over a stretching." *Nanoscale research letters* 6, no. 1 (2011): 1-10.
[52] Khashi'ie, Najiyah Safwa, Norihan Md Arifin, Ezad Hafidz Hafidzuddin, and Nadihah Wahi. "Mixed convective stagnation point flow of a thermally stratified hybrid Cu-Al2O3/water nanofluid over a Permeable stretching/shrinking sheet." *ASM Science Journal* 12, Special issue 5 (2019): 17-25.